

Superradiance in ultracold Rydberg atoms

Tun Wang,¹ R. Côté,¹ E. Eyler,¹ S. Farooqi,¹ P. Gould,¹ M. Koštrun,^{1,2} D. Tong,¹ D. Vranceanu,³ and S. F. Yelin^{1,2}

¹*Department Of Physics, University of Connecticut, Storrs, CT 06269*

²*ITAMP, Harvard-Smithsonian Center for Astrophysics, Cambridge, MA 02138*

³*Theoretical Division, Los Alamos National Laboratory, NM 87545*

(Dated: May 24, 2019)

Experiments in dense, ultracold rubidium Rydberg atoms show a considerable decrease of excited state lifetimes compared to dilute gases. We find that this accelerated decay could be explained by collective and cooperative effects, leading to superradiance. We use a novel formalism to calculate effective decay times in a dense Rydberg gas for all decay channels. We find that the tendency to decay into the lowest levels is inverted in dense gases and that the now-dominant low-frequency decays favor a superradiant decay mode.

In many-body physics, superradiance represents a fundamental multi-atom collective effect. In this paper, we are interested in collective effects connected to photon exchange between atoms. *Cooperative* effects, i.e., collective effects involving the exchange of virtual photons, can lead to the formation of so called Dicke states [1]. In these states, the symmetric superposition of all states with the same total excitation level if the atom number, N , is constant. Cooperative effects are therefore always coherent in nature and lead to superradiance. Interest in Dicke states has grown recently because of their potential advantages in quantum information processing [2] and their importance in the behavior of Bose-Einstein condensates [3].

Cooperative phenomena usually require very high atomic density. The boundary, however, between cooperative and non-cooperative collective effects in an intermediate density regime is smooth. In a dense atomic gas, speed-up of spontaneous decay, for example, can be due to purely incoherent causes, and is then aptly called “amplified spontaneous emission” (ASE). The difference between ASE and superradiance (or “superfluorescence”) is that ASE typically results in an increase of the radiant intensity which is still proportional to N , the number of atoms. The signature of superradiant decay, on the other hand, is an N^2 -dependence, which results in particular in an initial build-up of the emission intensity instead of its approximately exponential decrease for ASE. Most practical examples of “superradiance” will exhibit both cooperative and non-cooperative collective behavior. In this article, we therefore arbitrarily set the border between superradiance and ASE by using the initial slope of the decay intensity vs. time: If it is positive, we call it “superradiance”, otherwise, “ASE.” This way, the N^2 -vs. N -dependence of the intensity is indirectly taken into account; if the cooperative behavior is stronger, the intensity will initially grow, if the non-cooperative behavior is stronger, the intensity will monotonically decrease.

The difficulty of calculating effects including atom-atom cooperation has been the intractably large number of interconnected degrees of freedom, even if just a few particles are involved. To explore these collective effects,

many new ideas, such as the quantum jump approach, were developed to treat superradiance [4]. Recently, we successfully incorporated cooperative effects into our novel formalism for optically dense media. The result is a two-atom master equation for superradiance [5, 6, 7]. From the simplest version of this calculation we were able to obtain close agreement with observed signatures of superradiance including the effects of dissipation and the unique temporal build-up of a sharp flash of radiation. Moreover, our new formalism allows for easy incorporation of more complicated level structures, additional fields, and polarization effects.

Rydberg atoms have many special properties: their size can become comparable to the atomic separation; and they have huge dipole moments $\varphi \sim n^2$, where n is the principal quantum number of the Rydberg state. Indeed, the maximum length within which atoms can cooperate to superradiate, the so-called cooperative length $l_c = 2 \left(\frac{c}{N\gamma\lambda^2} \right)^{1/2}$ [8], where N is the density of atoms, λ is the transition wavelength, and γ the vacuum decay rate, is large for Rydberg atoms, which means superradiance or ASE should be easier to obtain than for ground state atoms [8]. This was confirmed in earlier experiments for Rydberg atoms at high temperatures [9, 10]. Therefore, these many-body effects may pose a limit on the measurement of lifetimes of Rydberg atoms [11] and may cause an undesirable frequency shift, for example, in atomic clocks [12].

The details for this formalism are described in [5, 6] so that we only mention here the methods and approximations made. In a dense atomic cloud, by arbitrarily choosing two probe atoms, the degrees of freedom of the surrounding atoms and the radiation fields can be formally eliminated by assuming Gaussian (and therefore classical) statistics of the light fields, and making a Markov approximation. This results in a two-atom master equation that includes up to second order quantum corrections, such as dipole-dipole interactions and cooperative effects due to atom-photon interaction with real or virtual photons. At this point, atomic collisions and center-of-mass motion are not included. In addition, the

sample size chosen has to be small, so that retardation effects can be neglected. It does not have to be, however, smaller than the cubic wavelength as is necessary for pure Dicke superradiance [13]. Neglecting the retardation effect can be justified because the amount of time it takes for light to propagate through the sample (which is of the order of 10^{-10} s for the sample sizes studied here) is significantly smaller than any other time spent in the system, in particular, the superradiant build-up and decay times (see, e.g., Fig. 1).

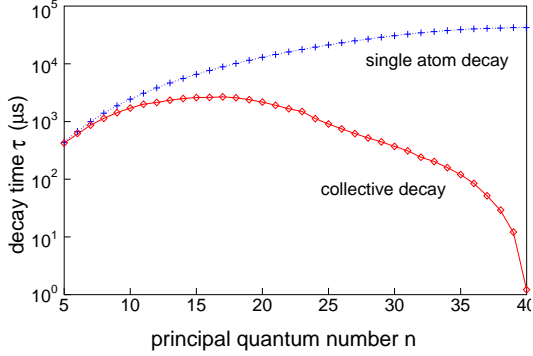


FIG. 1: Decay times from 40P to various nS states (\diamond) in a dense gas ($\mathcal{N} = 5 * 10^8 \text{ cm}^{-3}$) and in vacuum ($+$).

Following the discussion above, the master equation for a two-atom two-level system described by a density matrix ρ is given by [5]:

$$\begin{aligned} \dot{\rho} = & -\frac{i}{\hbar} [H_0, \rho] - \frac{1}{2} \sum_{i,j=1,2} \Gamma_{i,j} \left([\rho \sigma_i, \sigma_j^\dagger] + [\sigma_i, \sigma_j^\dagger \rho] \right) \\ & - \frac{1}{2} \sum_{i,j=1,2} (\Gamma_{i,j} + \gamma_{i,j}) \left([\rho \sigma_j^\dagger, \sigma_i] + [\sigma_j^\dagger, \sigma_i \rho] \right), \end{aligned} \quad (1)$$

where the Hamiltonian H_0 is an effective two-atom two-level Hamiltonian containing additional effects such as collisions, and which we set to zero here. The operator σ_i , $i = 1, 2$, is an atomic dipole lowering operator, $\sigma_i = (|b\rangle\langle a|)_i$ where $|a\rangle$ and $|b\rangle$ are the single atom excited and ground state, respectively. The operators $\Gamma_{i,j}$ in Eq. (1) are the most important ingredients, and their detailed calculation is given in [5] under simplifying assumptions of a homogeneous spherical sample. Here we just note that they include different electric field cumulants and list the final result: $\Gamma_{i,j} \delta(t-t') = \langle\langle E_i(t) E_j(t') \rangle\rangle$, where E_i denotes the quantum field. $\gamma_{i,j} \approx \gamma \delta_{ij}$, with γ the vacuum single atom decay rate and the Kronecker symbol δ_{ij} . With these simplifications in notation, Eq. (1) becomes an ordinary differential equation for linear combinations of matrix elements of ρ :

$$\dot{a} = -(2\Gamma + \gamma)a + \Gamma, \quad (2a)$$

$$\dot{m} = -2(2\Gamma + \gamma)n - 2\gamma(2a - 1) + 8\bar{\Gamma}x, \quad (2b)$$

$$\dot{x} = -(2\Gamma + \gamma)x + \bar{\Gamma}n. \quad (2c)$$

The quantities a , m , and x are expressed in terms of matrix elements $\rho_{\alpha\beta,\gamma\delta} \equiv \langle \alpha_i \gamma_j | \rho | \beta_i \delta_j \rangle$ where the α_i, \dots denote the level $|a\rangle$ or $|b\rangle$ of atom i , etc. Then a is the average excited population per atom, $a(t) = \rho_{aa,aa}(t) + \frac{1}{2}(\rho_{aa,bb}(t) + \rho_{bb,aa}(t))$; m is the effective inversion per atom, $n(t) = \rho_{aa,aa}(t) - \rho_{aa,bb}(t) - \rho_{bb,aa}(t) + \rho_{bb,bb}(t)$; and x is the correlation (of two atoms) per atom, $x(t) = (\rho_{ab,ba}(t) + \rho_{ba,ab}(t))/2$. The quantities $\Gamma_{i,i} = \Gamma$ and $\Gamma_{i \neq j} = \bar{\Gamma}$ are assumed to be approximately the same over the sample of atoms and can be expressed as

$$\begin{aligned} \Gamma &= \gamma \frac{a(t)}{2a(t) - 1} (e^{2\zeta} - 1) + 2\gamma \mathcal{C}^2 \varrho^4 \frac{\gamma}{\Gamma + \gamma/2} x(t) I(\zeta, \varrho) \\ \bar{\Gamma} &= 3\gamma \mathcal{C} \varrho \frac{\gamma}{\Gamma + \gamma/2} a(t) I(\zeta, \varrho) + 2\gamma \mathcal{C}^2 \varrho^4 \frac{\gamma}{\Gamma + \gamma/2} x(t) I(\zeta, \varrho) \end{aligned}$$

where

$$\begin{aligned} \zeta &= \frac{1}{2} \mathcal{C} \varrho \frac{\gamma}{\Gamma + \gamma/2} (2a(t) - 1) \\ I(\zeta, \varrho) &= \left| \frac{e^\xi (1 - \xi) + 1}{\xi^2} \right|_{\xi=\zeta+i\varrho}^2. \end{aligned}$$

In this simplified case, there are only two parameters: $\mathcal{C} = \mathcal{N} \lambda^3 / 4\pi^2$ is the cooperativity parameter or relative density, denoting the number of atoms per cubic wavelength; $\varrho = \pi d / \lambda$ is the sample size relative to the wavelength. Here, \mathcal{N} is the density of atoms, d is the average diameter of the sample, λ is the transition wavelength, and c is the speed of light in vacuum.

For our approach, the radiative interaction of an atom with itself is represented by Γ , while interactions with other atoms are represented by $\bar{\Gamma}$. If there were no cross-correlation between the atoms ($x = 0$), Γ would play the role of a completely incoherent repump. In this case, speed-up of decay for the inverted state would result in ASE, and in the non-inverted state, the slow-down of the decay would result in radiation trapping [6]. A non-zero cross-correlation ($x \neq 0$), however, as in our case, would lead to cooperative effects: collective dipoles would build up, thereby increasing Γ by the component responsible for superradiance. This leads to a rapid increase of intensity to a maximum proportional to N^2 , which is commonly the signature for superradiance. $\bar{\Gamma}$ couples the cross-correlation x to the population equations for m and a . Thus, our approach differs from traditional approaches since Γ and $\bar{\Gamma}$ contain both a coherent and an incoherent (or virtual and real) part of the dipole-dipole interaction.

To motivate our calculation, we first look at preliminary experimental results in Rydberg atoms. Rb atoms were trapped and cooled to 100 μK . Next, they were selectively excited by a pulsed UV laser to the 43p state. After delay time τ , all atoms in states with the principal quantum number $n \geq 27$ were Stark ionized. Free ions were detected separately and their number was observed to increase with delay, reaching 190 for a delay

of 35 μs . As depicted in Fig. 2, the number of ultracold atoms in Rydberg states with $n \geq 27$ decays fast, an estimated 10-100 times faster than measured in vacuum [18]. One potential source of this speed-up is the presence of amplified spontaneous emission or superradiance [9, 10, 14]. (One alternative explanation, so-called avalanche plasma formation, where all the initial Rydberg atoms would be ionized, can be discarded because after the longest measured delay there are always less than 200 ions present.) The remainder of this paper ad-

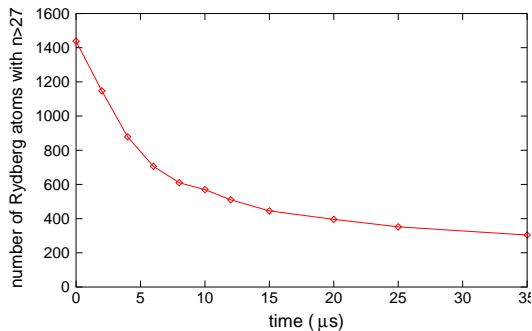


FIG. 2: Decay of number of atoms in Rydberg states with $n \geq 27$ following excitation to $n = 43p$. The initial density of Rydberg atoms in the experiment is $5 * 10^8 \text{cm}^{-3}$

dresses the possibility of superradiance in such ultracold Rydberg gases, and tries to compare the numerical calculations with experimentally measurable results. It is our intention to show that Eqs. (2) qualitatively demonstrate that the results seen in the experiment [15] could, in fact, be due to superradiance. The density of Rydberg atoms in the calculation is chosen to be the same as in the experiment, $\mathcal{N} = 5 * 10^8 \text{cm}^{-3}$. It is important to note that in the experiment, the geometry of the sample is cigar-shaped. Although this is an important experimental fact for achieving superradiance, because of mode selection with regard to directionality, we assume in the calculation a spherically-shaped sample for simplicity.

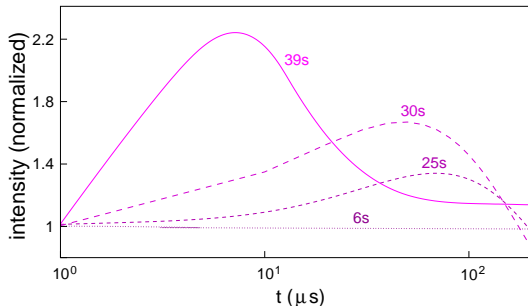


FIG. 3: The output intensity as function of time for a sample with density $5 * 10^8 \text{cm}^{-3}$ for the transition from state $40p$ to $39s$, $30s$, $25s$, and $6s$, respectively. For readability, the starting intensities are scaled to 1. In reality, they would scale with the number of atoms per wavelength.

The simulations presented here assume Rb atoms in the initial state of $40p$, exemplifying a range of possible initial states, such as $43p$. In Fig. 3 we show the decay from $40p$ into ns . In Fig. 1, the effective decay times are compared for a dense gas and in a vacuum (cf. [16]). In vacuum, the effective decay time τ_{eff} is the inverse of the Einstein A-coefficient. Clearly, in a vacuum the transition into the states with lowest n is fastest, and therefore decay into these channels is most likely. But this tendency is reversed in dense gases: the effective decay time for each transition is shorter than that in a vacuum or dilute gases. Since the collective and cooperative effects responsible for this speed-up depend only on the density relative to the wavelength cubed, the acceleration of the decay is obviously stronger for longer wavelengths. One of the main results of this letter is that the low-frequency decay becomes faster and more likely at higher densities, surpassing high-frequency decay at the densities studied here.

In Fig. 3, the intensity of some selective decays is shown over time. Because of energy conservation, the intensity must be proportional to the negative time derivative of the upper state population. (We neglect here all time-delay effects, resulting in an instantaneous intensity at time $t = 0$.) For the long-wavelength cases, an initially increasing intensity is achieved. This is the signature for superradiance as defined earlier in this article.

In order to get a general overview of which combinations of parameters lead to superradiance, we created a map in the $\mathcal{C} - \rho$ parameter space. Fig. 4 shows the border between superradiant and ASE behavior. This figure was created by testing different parameter combinations using the aforementioned formalism (Eqs. 2), and defining the border between the two regions by the slope of the decay intensity over time: if the initial slope is positive, superradiance outweighs ASE and vice versa. The selective decay from the $40P$ Rydberg state of Rb into all possible lower nS states is added to the map. We see that superradiant behavior is expected for decay into levels with $n \geq 22$.

Thus, we have found that dense excited atoms are much more likely to decay into long-wavelength channels, as compared to atoms in dilute gases. Since these channels could exhibit superradiant behavior (see Fig. 4), we have found that the combination of highly excited Rydberg atoms and relatively high densities can indeed lead to superradiance. Preliminary experimental results are consistent with our order-of-magnitude estimate for these effects.

To quantitatively compare the calculation to the experiment, a many channel calculation must be performed. When calculating all effective decay times for all transitions that can be achieved from a starting point, say, $40P$, branching ratios can be found and therefore the whole decay cascade determined. This is, however, beyond the scope of this paper. Our only intention is to make a sim-

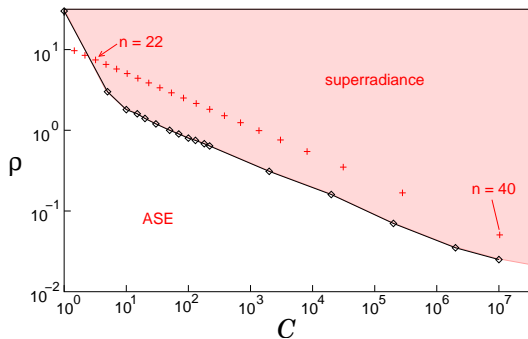


FIG. 4: Map of critical parameters of C and ρ (\diamond). Above the critical curve (shaded area) are the parameters for which superradiance happens. Also shown are the C and ρ for the decay to nS states from 40P state (+). Density of atoms is the same as above.

ple estimate of the total lifetime of the 40P state, and compare it to the lifetime of the Rb atom in the $n = 27$ to $n = 40$ state range of about $11\mu\text{s}$ (see Fig. 2). The lifetime can be estimated by adding up all decay rates:

$$\frac{1}{\tau_{\text{total}}} = \sum_n \frac{1}{\tau_{\text{eff}}}, \quad (3)$$

where we sum over the range of levels $n = 5$ to $n = 40$ for s and $n = 5$ to $n = 39$ for d states. The result is $\tau_{\text{total}} \approx 5\mu\text{s}$. While it is not possible to compare this number directly to the data in Fig. 2, we can calculate the theoretical lifetime for the $40p$ state in vacuum. In this case, we find (cf. data in Fig. 1) $\tau_{\text{total},0} \approx 210\mu\text{s}$, which suggests a forty-fold speed-up for the decay of Rydberg atoms in the range of $n = 40$ in the density range studied. This number is consistent with the estimated 10-100 fold faster time-scale as seen experimentally in Fig. 2.

In this article, we discussed the possibility of superradiant decay in cold gases of Rydberg atoms at densities of $10^8 - 10^9\text{ cm}^{-3}$. Superradiance could occur because lower-frequency decays are increasingly more likely to happen in denser gases, and they contribute most to cooperative behavior. This type of superradiance may even be useful for selective and accelerated decay along certain paths.

We neglected black body radiation, since it is important for superradiance only for the initiation of the radiation process at most, provided $N \gg n_B$, where n_B is the average number of black body photons per mode at the frequency of transitions [17]. In addition, the possibility of mode competition and interference between different

decay channels is neglected for simplification. In future work, the effects of geometry, in particular, the aspect ratio of the gases, should be taken into account. In practice, only elongated samples are used to show superradiance [13].

In summary, results from recent experiments measuring the decay rates a of ultracold dense Rydberg Rb atoms, a few orders of magnitude higher than that of atoms in dilute gases, are consistent with superradiant behavior in the framework of our model.

The authors gratefully acknowledge the support from the National Science Foundation. DV wishes to thank DOE for support through the Los Alamos National Laboratories. We want to thank J. Riccobono for discussions.

-
- [1] R. Dicke, Phys. Rev. **93**, 99 (1953).
 - [2] J. M. Taylor, A. Imamoglu, and M. D. Lukin, Phys. Rev. Lett. **91**, 246802 (2003).
 - [3] S. Inouye, A. P. Chikkatur, D. M. Stamper-Kurn, J. Stenger, D. E. Pritchard, and K. W. Science **285**, 571 (1999).
 - [4] J. P. Clemens and H. J. Carmichael, Phys. Rev. A **65**, 023815 (2002).
 - [5] S. F. Yelin, M. Kostrun, T. Wang, and M. Fleischhauer, in preparation.
 - [6] M. Fleischhauer and S. F. Yelin, Phys. Rev. A **59**, 2427 (1999).
 - [7] S. F. Yelin and M. Fleischhauer, Opt. Exp. **1**, 160 (1997).
 - [8] F. F. Arecchi and E. Courtens, Phys. Rev. A **2**, 1730 (1970).
 - [9] F. Gounand, M. Hugon, P. R. Fournier, and J. Berlande, J. Phys. B **12**, 547 (1979).
 - [10] Y. Kaluzny, P. Goy, M. Gross, J. M. Raimond, and S. Haroche, Phys. Rev. Lett. **51**, 1175 (1983).
 - [11] A. L. de Oliveira, M. W. Mancini, V. S. Bagnato, and L. G. Marcassa, Phys. Rev. A **65**, 031401(R) (2002).
 - [12] D. E. Chang, J. Ye, and M. D. Lukin, Phys. Rev. A **69**, 023810 (2004).
 - [13] M. Gross and S. Haroche, Phys. Rep. **93**, 301 (1982).
 - [14] M. Trache, Opt. Comm. **79**, 99 (1990).
 - [15] S. M. Farroqi, D. Tong, S. Krishnan, J. Stanojevic, Y. P. Zhang, J. R. Ensher, A. S. Estrin, C. Boisseau, R. Côté, E. E. Eyler, et al., Phys. Rev. Lett. **91**, 183002 (2003).
 - [16] M. R. Flannery and D. Vrinceanu, Phys. Rev. A **68**, 030502(R) (2003).
 - [17] J. M. Raimond, P. Goy, M. Gross, C. Fabre, and S. Haroche, Phys. Rev. Lett. **49**, 1924 (1982).
 - [18] This factor is a conservative estimate at this time, and it will be quantified more exactly in an improved experimental setting.